Structural Eng./Earthquake Eng., JSCE, Vol. 15, No. 2, 165s—173s, 1998 July
(J. Struct. Mech. Earthquake Eng., JSCE, No. 598/ I —44)

A DEGENERATE FORMULATION FOR LARGE DISPLACEMENT ANALYSIS OF THREE-DIMENSIONAL SOLID BEAMS

Eiki YAMAGUCHI[1], Muhammad HAMMADEH[2] and Yoshinobu KUBO[3]

[1] Member of JSCE, Ph.D., Assoc. Professor, Dept. of Civil Eng., Kyushu Institute of Technology (Tobata, Kitakyushu 804-8550, Japan)
[2] Student Member of JSCE, M. Eng., Grad. School of Civil Eng., Kyushu Institute of Technology
[3] Member of JSCE, Dr. Eng., Professor, Dept. of Civil Eng., Kyushu Institute of Technology

A finite element formulation for the large displacement analysis of three-dimensional solid beams is proposed. It is based on the degeneration approach: the governing equations for a general solid are directly discretized. The assumptions of the Timoshenko beam theory are implemented in the discretization process by devising a 9-node beam element and utilizing the penalty method. The shear stiffness is adjusted by introducing two shear correction factors into the constitutive equations. The formulation is quite simple and straightforward, mainly because rotations are excluded from nodal variables. Several example problems are solved to demonstrate the validity of the present formulation.

Key Words : *three-dimensional solid beams, large displacement, degeneration approach, FEM*

1. INTRODUCTION

A three-dimensional beam formulation is not a simple extension of a two-dimensional formulation, since finite rotations that are not vector quantities must be accounted for in the three-dimensional analysis. Therefore, various techniques such as Euler angles and Rodrigues parameters have been devised: detailed description of this issue is available elsewhere[1), 2)]. Because of the complexity of dealing with finite rotations, various large displacement formulations/theories for three-dimensional beam analysis have been proposed, some of which are listed at the end of this paper[3)-17)]. Although they differ from each other, all the beam elements based on those formulations do possess rotations as nodal variables. At the current stage of development, a rigorous treatment of finite rotations is certainly possible, but such a class of formulation still appears to be rather involved and complicated inevitably.

Kanok-Nukulchai et al.[18)] have proposed a simple large deformation formulation for shell analysis. They have employed the degeneration approach, which directly discretizes the three-dimensional field equations for a general solid, and eliminated rotations from nodal variables of their shell element by introducing relative displacements. The simplicity of the formulation stems from the fact that no complicated treatment of finite rotations is needed. The same strategy has been taken successfully for the nonlinear analysis of two-dimensional beams[19), 20)].

The objective of the present research is to propose a simple yet accurate finite element formulation for the large displacement analysis of three-dimensional solid beams. To this end, we employ the degeneration approach and exclude rotations from nodal variables, so that the formulation is free from the difficulties associated with finite rotations. Only elastic beams are dealt with in the present study. The extension to an inelastic case is, however, straightforward, as we have already done in two-dimensional beam analysis[20)].

2. FORMULATION

We utilize two sets of coordinate systems in the present formulation: spatial coordinates and material coordinates[21)]. In what follows, x, y and z denote the former while X, Y and Z the latter. The tensor notation is also employed in the present description, so that we may use x_i and X_I to represent spatial coordinates and material coordinates, respectively. Furthermore, we let the lower-case and upper-case

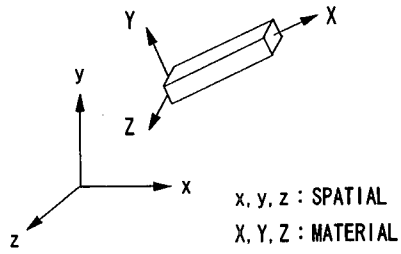

Fig. 1 Coordinate systems

subscripts designate the association with the spatial and material coordinate systems, respectively. We set the X (X_1)-axis passing through the centroid of every cross-section of a beam, as is shown in **Fig. 1**.

We resort to the total Lagrangian formulation in the present study[22]. Therefore, the description would be in terms of the 2nd Piola-Kirchhoff stress S_{IJ} and the Green strain E_{IJ}.

(1) Beam assumptions

The solid beams we consider in the present study are classified as the Timoshenko beam[23]. Namely, we employ the following beam assumptions:

a) cross sections do not deform;
b) plane cross-sections remain plane after deformation; and
c) only three stress components are significant.

Using the Green strain components, we can mathematically express Assumption a) as

$$E_{YY} = E_{ZZ} = E_{YZ} = 0 \tag{1}$$

Assumption b) is implemented by devising a new finite element, the details of which we shall describe in the subsequent section.

To be specific, Assumption c) means

$$S_{YY} = S_{ZZ} = S_{YZ} = 0 \tag{2}$$

The remaining stress components S_{XX}, S_{XY} and S_{XZ} are related to the three nontrivial strain components E_{XX}, E_{XY} and E_{XZ}, respectively, through Young's modulus E and the shear modulus G. Because of Assumption b), the shear correction factors (shear coefficients) need be introduced into the constitutive relations. This issue will be discussed later in the section 2.(3).

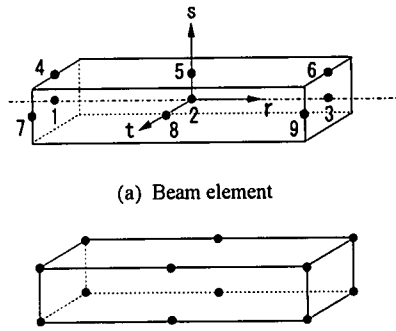

(a) Beam element

(b) 12-node solid element

Fig. 2 Finite elements

(2) Beam element

The beam element used in this study evolves from a 12-node three-dimensional isoparametric solid element. These two elements are illustrated in **Fig. 2**. The beam element consists of nine nodes: three reference nodes on the beam axis (Nodes 1 to 3) and six relative nodes on the beam surface (Nodes 4 to 9). The present beam element has only three nodes on a cross section, while the original solid element has four: we have eliminated one node so as to keep a plane cross-section plane, thus implementing Assumption b).

We assign three displacement components to each of the reference nodes as nodal variables while we assign to each relative node three components of the relative displacement with respect to the reference node located on the same cross-section. No rotations are involved explicitly and the relative displacements can be viewed as substitutes for them. Thus all the nodal variables are vector quantities in the present beam element. Consequently, the complexity due to finite rotations in the conventional beam elements is not an issue here at all.

We describe geometry of the beam element by a set of natural curvilinear coordinates (r,s,t), each of which has the range of -1 to 1, i.e. $-1 \le r,s,t \le 1$. The displacement vector u_j of a point at (r,s,t) in a beam element can be expressed in terms of nodal variables as

$$u_j = \sum_{a=1}^{9} N^a(r,s,t) U_j^a \tag{3}$$

where U_j^a denotes the absolute displacement vector at Node "a" for $a = 1 \sim 3$ and the relative displacement vector at Node "a" for $a = 4 \sim 9$. The shape function

N^a consistent with this definition of U_j^a is derived in the way similar to that of Ref. 18) and given by

$$N^a(r,s,t)=\begin{cases}\frac{1}{2}r^a r\left(1+r^a r\right) & \text{for } a=1,3\\ 1-r^2 & \text{for } a=2\\ \frac{1}{2}r^a r\left(1+r^a r\right)\left(s^a s+t^a t\right) & \text{for } a=4,6,7,9\\ \left(1-r^2\right)\left(s^a s+t^a t\right) & \text{for } a=5,8\end{cases} \tag{4}$$

where

$$r^a=\begin{cases}-1 & \text{for } a=1,4,7\\ 0 & \text{for } a=2,5,8\\ 1 & \text{for } a=3,6,9\end{cases}$$
$$s^a=\begin{cases}0 & \text{for } a=1\sim 3,7\sim 9\\ 1 & \text{for } a=4\sim 6\end{cases} \tag{5}$$
$$t^a=\begin{cases}0 & \text{for } a=1\sim 6\\ 1 & \text{for } a=7\sim 9\end{cases}$$

It is noted that because of the employment of the relative nodes, the representation of rigid-body displacement is ensured by $\sum_{a=1}^{3} N^a = 1$.

This element is isoparametric provided that relative position vector is input for each relative node. The relative position vector is therefore defined in the same way as the relative displacement vector and we have

$$x_j=\sum_{a=1}^{9} N^a(r,s,t)X_j^a \tag{6}$$

where X_j^a with $a=1\sim 3$ is the position vector of a reference node while X_j^a with $a=4\sim 9$ is the relative position vector of a relative node with respect to the reference node located on the same cross-section.

(3) Shear correction factors

Assumption b) implies constant shear strain over a cross section when a beam undergoes bending behavior. This simplifies analysis, however the predicted deformation appears to be slightly different from a real state. To overcome this problem, a shear correction factor has been introduced in the Timoshenko beam theory[23),24)].

Assumption b) suppresses the warping of a cross section and tends to overestimate the torsional rigidity[25)]. In fact, the assumption leads to the torsional constant equal to the polar moment of inertia. The adjustment of the torsional rigidity is therefore required, which will be achieved in the present study by introducing another shear correction factor into the stress-strain relationships.

Consequently, the constitutive equations are assumed to take the following form in the present formulation:

$$\begin{aligned}S_{XX}&=EE_{XX}\\ S_{XY}&=2\alpha GE_{XY}^{EY}+2\beta GE_{XY}^{OY}\\ S_{XZ}&=2\alpha GE_{XZ}^{EZ}+2\beta GE_{XZ}^{OZ}\end{aligned} \tag{7}$$

where α and β are the shear correction factors. The superscripts EY and OY indicate the even part and the odd part with respect to the Y-axis, respectively. To be specific, E_{XY}^{EY} and E_{XY}^{OY} at a point (X,Y,Z) in an element are defined as

$$\begin{aligned}E_{XY}^{EY}(X,Y,Z)&=\frac{1}{2}\left[E_{XY}(X,Y,Z)+E_{XY}(X,Y,-Z)\right]\\ E_{XY}^{OY}(X,Y,Z)&=\frac{1}{2}\left[E_{XY}(X,Y,Z)-E_{XY}(X,Y,-Z)\right]\end{aligned} \tag{8}$$

Likewise, we define E_{XZ}^{EZ} and E_{XZ}^{OZ} as

$$\begin{aligned}E_{XZ}^{EZ}(X,Y,Z)&=\frac{1}{2}\left[E_{XZ}(X,Y,Z)+E_{XZ}(X,-Y,Z)\right]\\ E_{XZ}^{OZ}(X,Y,Z)&=\frac{1}{2}\left[E_{XZ}(X,Y,Z)-E_{XZ}(X,-Y,Z)\right]\end{aligned} \tag{9}$$

Since the even part and the odd part of the shear strain are related to bending deformation and torsional deformation respectively, the shear correction factor α is associated with the deflection due to shear deformation while the other shear correction factor β with the torsional rigidity. The value of α can be determined by the shape of the cross section whereas the value of β takes the ratio of the torsional constant to the polar moment of inertia.

(4) Governing discretized equations

The boundary value problem that we are to solve is defined by the following equations together with Eq. (7)[21),22)].

$$(S_{IJ}F_{jJ})_{,I} + \rho_0 b_j = 0 \quad \text{in } V_0 \tag{10}$$

$$E_{IJ} = \frac{1}{2}\left(F_{kI}F_{kJ} - \delta_{IJ}\right) \text{ in } V_0 \tag{11}$$

$$t_{0j} = n_{0I}S_{IJ}F_{jJ} \quad \text{on } A_{0t} \tag{12}$$

$$\bar{u}_j = u_j \quad \text{on } A_{0u} \tag{13}$$

where F_{jJ} is the deformation gradient, ρ_0 the mass density, b_j the body force, δ_{IJ} the Kronecker delta, t_{0j} the prescribed traction, n_{0I} the unit normal vector on the boundary surface and $\bar{u}_j$ the prescribed displacement. V_0 is the body under consideration, A_{0t} the boundary surface with the prescribed traction and A_{0u} the boundary surface with the prescribed displacement. The subscript 0 indicates the original state. Eq. (10) is the equilibrium equation, Eq. (11) the definition of the Green strain, Eq. (12) the mechanical boundary condition and Eq. (13) the geometrical boundary condition. In addition to these governing equations, we have to take into account the constraints of Eq. (1) in the present boundary value problem.

For the basis of finite element formulation, we employ the principle of virtual work derived from Eqs. (10) to (13)[22]. In order to impose Eq. (1), we further resort to the penalty method[26]. Hence, we start the formulation with the following equation:

$$\begin{aligned} W = &\int_{V_0} S_{XX}\delta E_{XX}dV + \int_{V_0} 2S_{XY}\delta E_{XY}dV \\ &+ \int_{V_0} 2S_{XZ}\delta E_{XZ}dV - \int_{V_0} \rho_0 b_j \delta u_j dV \\ &- \int_{A_{0t}} t_{0j}\delta u_j dA + \int_{V_0} kE_{YY}\delta E_{YY}dV \\ &+ \int_{V_0} kE_{ZZ}\delta E_{ZZ}dV + \int_{V_0} kE_{YZ}\delta E_{YZ}dV = 0 \end{aligned} \tag{14}$$

where δE_{IJ}, δu_j and k are the virtual strain, the virtual displacement and the penalty number, respectively.

For δu_j, we employ the same shape functions as those for u_j, so that we have

$$\delta u_j = \sum_{a=1}^{9} N^a \delta U_j^a \tag{15}$$

where δU_j^a is the nodal virtual displacement defined in the same way as U_j^a. Substituting Eq. (15) into Eq. (14), we obtain

$$W = \sum_{e=1}^{n} W^e = 0 \tag{16}$$

where

$$W^e = \sum_{b=1}^{9} \delta U_j^b \left[K_j^b - R_j^b\right] \tag{17}$$

$$\begin{aligned} K_j^b = \int_{V_0^e} &[S_{XX}F_{jX}N_{,X}^b \\ &+ S_{XY}(F_{jX}N_{,Y}^b + F_{jY}N_{,X}^b) \\ &+ S_{XZ}(F_{jX}N_{,Z}^b + F_{jZ}N_{,X}^b) \\ &+ kE_{YY}F_{jY}N_{,Y}^b + kE_{ZZ}F_{jZ}N_{,Z}^b \\ &+ \frac{1}{2}kE_{YZ}(F_{jY}N_{,Z}^b + F_{jZ}N_{,Y}^b)]dV \end{aligned} \tag{18}$$

$$R_j^b = \int_{V_0^e} \rho_0 b_j N^b dV + \int_{A_{0t}^e} t_{0j}N^b dA \tag{19}$$

n in Eq. (16) stands for the number of elements. For finite element analysis, it is more convenient to rewrite Eqs. (18) and (19) in matrix form:

$$\mathbf{K}^b = \int_{V_0^e} \mathbf{F}\mathbf{S}\mathbf{A}^b dV \tag{20}$$

$$\mathbf{R}^b = \int_{V_0^e} \rho_0 N^b \mathbf{b} dV + \int_{V_0^e} N^b \mathbf{b} dV \tag{21}$$

where

$$\mathbf{F} = \begin{bmatrix} F_{xX} & F_{xY} & F_{xZ} \\ F_{yX} & F_{yY} & F_{yZ} \\ F_{zX} & F_{zY} & F_{zZ} \end{bmatrix} \tag{22}$$

$$\mathbf{S} = \begin{bmatrix} S_{XX} & S_{XY} & S_{XZ} \\ S_{XY} & kE_{YY} & kE_{YZ}/2 \\ S_{XZ} & kE_{YZ}/2 & kE_{ZZ} \end{bmatrix} \tag{23}$$

$$\left(\mathbf{A}^b\right)^T = \begin{bmatrix} N_{,X}^b & N_{,Y}^b & N_{,Z}^b \end{bmatrix} \tag{24}$$

$$\mathbf{b}^T = \begin{bmatrix} b_x & b_y & b_z \end{bmatrix} \tag{25}$$

We evaluate Eqs. (18) and (19) (or, equivalently, Eqs. (20) and (21)) for each element, and then assemble all those individual element contributions. The summation symbol with e in Eq. (16) represents this assemblage procedure. Since the nodal virtual displacement is arbitrary, we end up with

$$\mathbf{K}-\mathbf{R}=\mathbf{0} \tag{26}$$

where $\mathbf{K}$ and $\mathbf{R}$ are the assemblage of K_j^b and R_j^b, respectively.

Since Eq. (26) is a nonlinear algebraic system, we must have recourse to some numerical methods. In the present study, we utilize the Newton-Raphson technique, so that the following linearized equation is solved repeatedly until convergence is attained:

$$\mathbf{K_T}\Delta\mathbf{U}^{(m)}=\mathbf{R}-\mathbf{K}^{(m)} \tag{27}$$

where the superscript (m) denotes the number of iterations. $\Delta\mathbf{U}^{(m)}$ is the iterative increment of the nodal displacement at the mth iteration. $\mathbf{K_T}$ is the tangent stiffness matrix, which can be evaluated by taking the derivative of $\mathbf{K}$ with respect to the nodal displacement $\mathbf{U}$. To that end, consistent linearization[18),27)] is performed and the tangent stiffness matrix is obtained for an element as

$$\mathbf{K}_{\mathbf{T}}^{ba}=\frac{\partial\mathbf{K}^b}{\partial\mathbf{U}^a}$$
$$=\int_{V_0^e}(\mathbf{B}^b)^T\mathbf{D}\mathbf{B}^a dV+\left[\int_{V_0^e}(\mathbf{A}^b)^T\mathbf{S}\mathbf{A}^a dV\right]\mathbf{I} \tag{28}$$

where

$$\mathbf{B}^b=\begin{bmatrix} F_{xX}N_{,X}^b \\ F_{xY}N_{,Y}^b \\ F_{xZ}N_{,Z}^b \\ F_{xY}N_{,Z}^b+F_{xZ}N_{,Y}^b \\ (F_{xX}N_{,Y}^b+F_{xY}N_{,X}^b)^{EY} \\ (F_{xX}N_{,Y}^b+F_{xY}N_{,X}^b)^{OY} \\ (F_{xX}N_{,Z}^b+F_{xZ}N_{,X}^b)^{EZ} \\ (F_{xX}N_{,Z}^b+F_{xZ}N_{,X}^b)^{OZ} \end{bmatrix}$$

$$\begin{bmatrix} F_{yX}N_{,X}^b & F_{zX}N_{,X}^b \\ F_{yY}N_{,Y}^b & F_{zY}N_{,Y}^b \\ F_{yZ}N_{,Z}^b & F_{zZ}N_{,Z}^b \\ F_{yY}N_{,Z}^b+F_{yZ}N_{,Y}^b & F_{zY}N_{,Z}^b+F_{zZ}N_{,Y}^b \\ (F_{yX}N_{,Y}^b+F_{yY}N_{,X}^b)^{EY} & (F_{zX}N_{,Y}^b+F_{zY}N_{,X}^b)^{EY} \\ (F_{yX}N_{,Y}^b+F_{yY}N_{,X}^b)^{OY} & (F_{zX}N_{,Y}^b+F_{zY}N_{,X}^b)^{OY} \\ (F_{yX}N_{,Z}^b+F_{yZ}N_{,X}^b)^{EZ} & (F_{zX}N_{,Z}^b+F_{zZ}N_{,X}^b)^{EZ} \\ (F_{yX}N_{,Z}^b+F_{yZ}N_{,X}^b)^{OZ} & (F_{zX}N_{,Z}^b+F_{zZ}N_{,X}^b)^{OZ} \end{bmatrix} \tag{29}$$

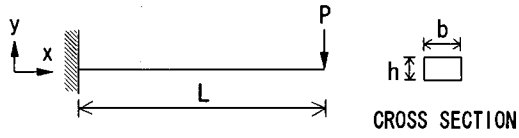

Fig. 3 Cantilever beam under end load

$$\mathbf{D}=\begin{bmatrix} E & 0 & 0 & 0 & 0 & 0 & 0 & 0 \\ & k & 0 & 0 & 0 & 0 & 0 & 0 \\ & & k & 0 & 0 & 0 & 0 & 0 \\ & & & k/4 & 0 & 0 & 0 & 0 \\ & & & & \alpha G & 0 & 0 & 0 \\ & & & & & \beta G & 0 & 0 \\ & sym. & & & & & \alpha G & 0 \\ & & & & & & & \beta G \end{bmatrix} \tag{30}$$

and $\mathbf{I}$ is the identity matrix.

3. NUMERICAL EXAMPLES

Numerical examples are solved to test the effectiveness of the proposed formulation. The Gauss scheme of $2\times2\times2$ is employed for numerical integrations in the example problems. All the calculations are performed on Sun SPARCstation 2 using double precision, and the Euclidean norm of incremental displacements less than 10^{-9} times the current displacement norm is used as the condition for convergence. In the following presentation, we denote the free-end displacements in the x-, y- and z-directions by u, v and w, respectively, and we let I designate the moment of inertia of a cross section with respect to the minor axis.

(1) Cantilever beam under end load

This is a well-known benchmark problem and depicted in **Fig. 3**. The dimensions and material properties are assumed as: $L=100$; $h=1$; $b=12$; $E=2\times10^6$; and $\alpha G=1\times10^6$. Only a planar behavior in the $x-y$ plane occurs, so that the value of β has no influence on the numerical results.

The effect of the penalty number k is explored first. To this end, the analysis of the cantilever using five beam elements is conducted for various values of k. The deflections at the free end are presented in **Table 1**. We observe from the table that v converges as the value of k increases, and that 10^3 times Young's

Table 1 Effect of the penalty number k (cantilever beam)

k / E	$-v / L$	
	$PL^2 / EI = 4$	$PL^2 / EI = 10$
10^0	.66784	.80614
10^1	.66769	.80593
10^2	.66767	.80591
10^3	.66767	.80590
10^4	.66767	.80590
10^5	.66767	.80590

Table 2 Free-end deflections due to various discretizations (cantilever beam)

	$-v / L$				
PL^2/EI	Anal.[28]	3 elem.	5 elem.	10 elem.	25 elem.
2	.49346	.49039	.49242	.49323	.49345
4	.66996	.66323	.66767	.66945	.66993
6	.74457	.73522	.74135	.74385	.74453
8	.78498	.77352	.78098	.78409	.78493
10	.81061	.79734	.80590	.80956	.81055

modulus E appears sufficiently large to achieve convergence. Hence, $k = 10^3 E$ is to be employed in the present study hereafter.

The analytical solution of this problem by means of elliptic integrals is available[28]. We examine the performance of the proposed formulation against this analytical solution. The numerical results due to several discretizations are summarized in **Table 2**. The values are clearly improved as the number of elements increases: the discrepancies of the results with 25 elements from the respective analytical solutions are all less than 0.01%. Even by five elements we have obtained the results within the difference of 1%, which seems good enough from a practical point of view. The load-displacement curve due to five elements is shown together with the reference solutions in **Fig. 4**.

(2) Buckling of a cantilever column

We analyze a cantilever column shown in **Fig. 5**. Three different cases, Columns I to III, are considered: Columns I and II are prismatic with $b = 12$, but the width of Column III is assumed to vary continuously from $b = 6$ at the top of the column to $b = 12$ at the bottom in a parabolic fashion. The difference between Columns I and II lies in the shear modulus: $\alpha G = 1 \times 10^6$ for Column I and $\alpha G = 1 \times 10^3$ for Column II. For Column III, $\alpha G = 1 \times 10^6$ is assumed. The other conditions, common to all the three analyses, are: $L = 100$; $h = 1$; and $E = 2 \times 10^6$. The deflection

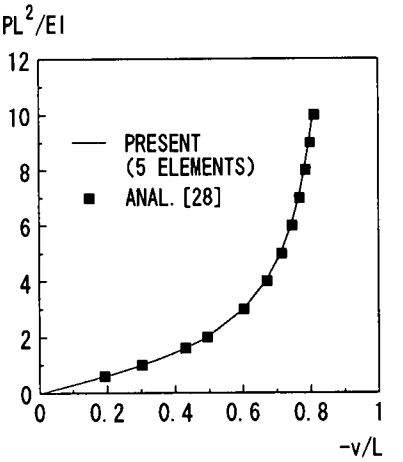

Fig. 4 Load-displacement relationship (cantilever beam)

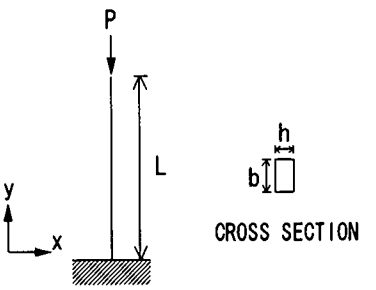

Fig. 5 Cantilever column (buckling problem)

would be confined in the $x - y$ plane, so that the value of β has no influence on the numerical results. The columns are tilted initially with a slope of 1:2000 to initiate the deflection in the $x - y$ plane.

As is known well, the critical load for the buckling of Column I is[24]

$$P_{crI} = \frac{\pi^2 EI}{4L^2} \tag{31}$$

Since the shear modulus of Column II is small, the critical load reduces to[24]

$$P_{crII} = \frac{P_{crI}}{1 + P_{crI} / \alpha GA} = 0.961 P_{crI} \tag{32}$$

where A is the cross-sectional area. The moment of inertia of Column III varies and is defined by

$$I(\xi) = I_0 \left(1 + \frac{\xi}{241.42}\right)^2 \tag{33}$$

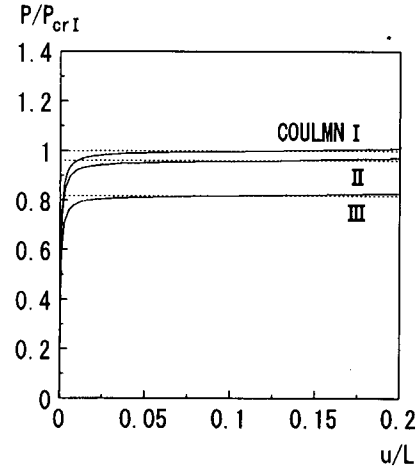

Fig. 6 Load-displacement curves (Columns I to III)

where ξ is the distance from the top of the column, and I_0 is the moment of inertia at $\xi = 0$, that is, at the top of the column. The critical load of Column III is then given by[24]

$$P_{crIII} = \frac{2.023EI(100)}{L^2} = 0.820P_{crI} \qquad (34)$$

Each column is discretized by five elements and analyzed. It is noted that with the present beam elements we can model the varying cross-section of Column III as it is. The load-displacement curves are drawn in **Fig. 6**, which shows that the deflections in all the three cases increase very rapidly in the vicinity of the respective critical loads indicated by the dotted lines.

For Column I, the post-buckling behavior has been obtained analytically[24]. In **Table 3**, the present numerical results are listed in comparison with the analytical solutions. Due to the initial slope, the numerical result overestimates the analytical value by about 3% at $P / P_{crI} = 1.015$. The discrepancy, however, diminishes quickly with the increase of the deflection; very good agreement is observed at the larger loads with the error much less than 1%.

(3) Lateral buckling of a cantilever beam

The cantilever beam shown in **Fig. 7** is analyzed. The conditions are: $L = 100$; $h = 12$; $b = 0.2$; $E = 2 \times 10^6$; $G = 1 \times 10^6$; $\alpha = 0.8333$; and $\beta = 0.01329$. In addition to the vertical load P, a small transverse load of $P / 2000$ is applied at the free end to initiate the out-of-plane displacement.

Table 3 Post-buckling behavior of Column I

P / P_{crI}	u / L	
	Anal.[24]	Present
1.015	.220	.227
1.063	.422	.421
1.152	.593	.592
1.293	.719	.717

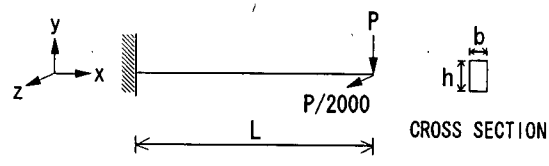

Fig. 7 Cantilever beam (lateral buckling problem)

While the transverse load is always applied at the centroid of the cross section, three different loading points are considered for the vertical load P. Accordingly, we analyze three beams, Beams A to C: P is applied at the centroid of the cross section in Beam A; at the top edge in Beam B; and at the bottom edge in Beam C.

The critical load for the lateral buckling of Beam A has been evaluated analytically as[24]

$$P_{crA} = \frac{4.013\sqrt{EIGJ}}{L^2} \qquad (35)$$

where J is the torsional constant. In the case of Beam B, the critical load reduces to[24]

$$P_{crB} = \left(1 - \frac{h/2}{L}\sqrt{\frac{EI}{GJ}}\right)P_{crA} = 0.958P_{crA} \qquad (36)$$

The critical load of Beam C is the largest[24]:

$$P_{crC} = \left(1 + \frac{h/2}{L}\sqrt{\frac{EI}{GJ}}\right)P_{crA} = 1.042P_{crA} \qquad (37)$$

We analyze these beams, each of which is discretized by five elements, and depict the load-transverse displacement relationships at the free end in **Fig. 8**, in which the critical loads are indicated by dotted lines. In each beam, a sharp increase of the displacement is clearly observed, as the critical load is approached.

(4) Cantilever 45-degree bend under end load

We consider the cantilever 45-degree circular bend illustrated in **Fig. 9**. The conditions are: $R = 100$;

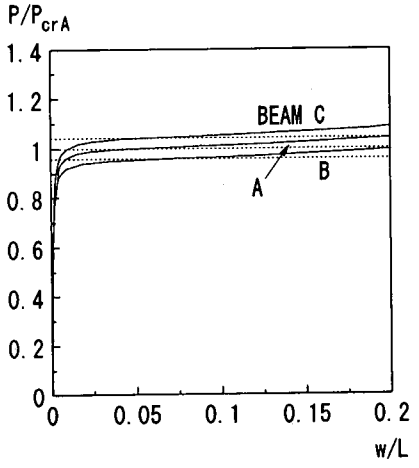

Fig. 8 Load-displacement curves (Beams A to C)

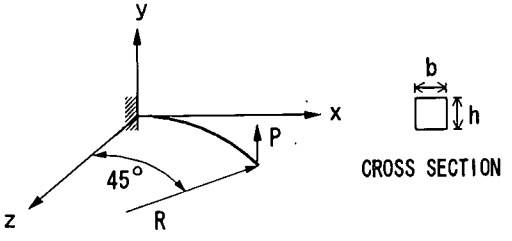

Fig. 9 Cantilever 45-degree circular bend

$b = h = 1$; $E = 1 \times 10^7$; $G = 0.5 \times 10^7$; $\alpha = 0.8333$; and $\beta = 0.8438$. The bend has been analyzed by many researchers[5), 10)-14), 16), 17)], but only Goto et al.[11)] have described explicitly the value of the torsional constant as $J = 0.1406$, from which the above value of β has been determined.

Using five elements, we analyze the bend and present the load-displacement curve together with the reference results in **Fig. 10**. **Table 4** provides a further comparison between the present results and those of Goto et al.[11)]. Very good agreement is observed with the difference well below 1%.

4. CONCLUDING REMARKS

A finite element formulation for the large displacement analysis of three-dimensional solid beams is presented. Due to the employment of the degeneration approach and the avoidance of rotations in nodal variables, nonlinear continuum mechanics could be applied directly, and the shear correction factors have been implemented to make up for the restrictions imposed by the beam assumptions. The formulation thus established is simple and straightforward. Accurate results have been obtained in the numerical examples, confirming the validity of the present formulation. We hence believe that the proposed procedure can serve as an attractive basis for the large displacement analysis of three-dimensional solid beams.

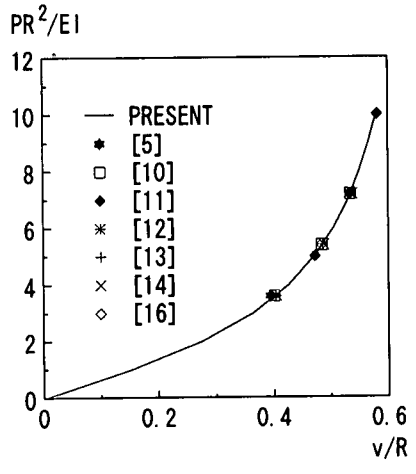

Fig. 10 Load-displacement relationship (45-degree bend)

Table 4 Free-end displacements (45-degree bend)

(a) $PR^2 / EI = 5$

	$-u/R$	v/R	$-w/R$
Present	.1018	.4711	.1733
Goto et al.[11)]	.1013	.4720	.1741

(b) $PR^2 / EI = 10$

	$-u/R$	v/R	$-w/R$
Present	.1681	.5791	.2941
Goto et al.[11)]	.1675	.5810	.2959

REFERENCES

1) Argyris, J.H.: An excursion into large rotations, *Comput. Meths. Appl. Mech. Engrg.*, Vol.32, pp.85-155, 1982.
2) Spring, K.W.: Euler parameters and the use of quaternion algebra in the manipulation of finite rotations: a review, *Mechanism Machine Theory*, Vol.21, pp.365-373, 1986.
3) Oran, C.: Tangent stiffness in space frames, *J. Struct. Div.*, ASCE, Vol.99, pp.987-1001, 1973.
4) Maeda, Y. and Hayashi, M.: Finite displacement analysis of space framed structures, *Proc. of JSCE*, No.253, pp.13-27, 1976 (in Japanese).
5) Bathe, K.J. and Bolourch, S.: Large displacement analysis of three-dimensional beam structures, *Int. J. Num. Meths. Engrg.*, Vol.14, pp.961-986, 1979.
6) Yoshida, Y., Masuda, N., Morimoto, T. and Hirosawa, N.: An incremental formulation for computer analysis of space framed structures, *Proc. of JSCE*, No.300, pp.21-31, 1980 (in Japanese).

7) Simo, J.C.: A finite strain beam formulation. The three-dimensional dynamic problem. Part I, *Comput. Meths. Appl. Mech. Engrg.*, Vol.49, pp.55-70, 1985.
8) Iura, M. and Hirashima, M.: Geometrically nonlinear theory of naturally curved and twisted rods with finite rotations, *Structural Eng./Earthquake Eng.*, JSCE, Vol.2, pp.353s-363s, 1985.
9) Maeda, Y and Hayashi, M.: Finite displacement theory of solid curved beams, *J. Struct. Engrg.*, JSCE, Vol.32A, pp.139-151, 1986 (in Japanese).
10) Simo, J.C. and Vu-Quoc, L.: A three-dimensional finite-strain rod model. Part II: Computational aspects, *Comput. Meths. Appl. Mech. Engrg.*, Vol.58, pp.79-116, 1986.
11) Goto, Y., Morikawa, Y. and Matsuura, S.: Direct Lagrangian nonlinear analysis of elastic space rods using transfer matrix technique, *Structural Eng./Earthquake Eng.*, JSCE, Vol.5, pp.151s-160s, 1986.
12) Dvorkin, E.N., Onate E. and Oliver J.: On a non-linear formulation for curved Timoshenko beam elements considering large displacement/rotation increments, *Int. J. Num. Meths. Engrg.*, Vol.26, pp.1597-1613, 1988.
13) Cardona, A. and Geradin, M.: A beam finite element non-linear theory with finite rotations, *Int. J. Num. Meths. Engrg.*, Vol.26, pp.2403-2438, 1988.
14) Crisfield M.A.: A consistent co-rotational formulation for non-linear three-dimensional beam-elements, *Comput. Meths. Appl. Mech. Engrg.*, Vol.81, pp.131-150, 1990.
15) Iwasaki, E. and Hayashi, M.: On the refinement of finite displacement analysis of space framed structures, *J. Struct. Engrg.*, JSCE, Vol.37A, pp.353-366, 1991 (in Japanese).
16) Crivelli, L.A. and Felippa, A.: A three-dimensional non-linear Timoshenko beam based on the core-congruential formulation, *Int. J. Num. Meths. Engrg.*, Vol.36, pp.3647-3673, 1993.
17) Goto, H., Kobayashi, H. and Iwakuma, T.: A simple finite displacement formulation using Eulerian angles, *J. Struct. Engrg.*, JSCE, Vol.43A, pp.333-338, 1997 (in Japanese).
18) Kanok-Nukulchai, W., Taylor, R.L. and Hughes, T.J.R.: A large deformation formulation for shell analysis by the finite element method, *Comput. & Structs.*, Vol.13, pp.19-27, 1981.
19) Yamaguchi, E., Kanok-Nukulchai, W. and Ohta, T.: A study on finite displacement analysis of beam structures by the finite element method, *J. Struct. Engrg.*, JSCE, Vol.35A, pp.175-183, 1989 (in Japanese).
20) Yamaguchi, E., Nishino, F. and Kubo, Y.: Nonlinear analysis of plane beams by means of degeneration approach, *J. Struct. Engrg.*, JSCE, Vol.43A, pp.31-39, 1997 (in Japanese).
21) Eringen, A.C.: *Continuum Physics*, Vols. I and II, Academic Press, New York, 1974.
22) Washizu, K.: *Variational Methods in Elasticity and Plasticity*, 3rd ed., Pergamon Press, New York, 1982.
23) Nishino, F. and Hasegawa, A.: *Elastic Analysis of Structures*, Gihoudou, Tokyo, 1983 (in Japanese).
24) Timoshenko, S.P. and Gere, J.M.: *Theory of Elastic Stability*, 2nd ed., McGraw-Hill, New York, 1961.
25) Simo, J.C. and Vu-Quoc, L.: A geometrically-exact rod model incorporating shear and torsion-warping deformation, *Int. J. Solids Structs.*, Vol.27, pp.371-393, 1991.
26) Hughes, T.J.R.: *The Finite Element Method*, Prentice-Hall, New Jersey, 1987.
27) Hughes, T.J.R. and Pister, K.S.: Consistent linearization in mechanics of solids and structures, *Comput. & Structs.*, Vol.8, pp.391-397, 1978.
28) Mattiason, K.: Numerical results from large deflection beam and frame problems analyzed by means of elliptic integrals, *Int. J. Num. Meths. Engrg.*, Vol.17, pp.145-153, 1981.

(Received September 5, 1997)

3次元充実断面梁の有限変位解析のためのディジェネレイト定式化

山口栄輝・ムハッマド ハッマデ・久保喜延

3次元充実断面梁の有限変位解析を行うための有限要素定式化を提案する．本定式化ではディジェネレイション法を採用し，固体力学の支配方程式を直接解く．解析対象とするのはティモシェンコ梁であり，その梁理論における仮定は，離散化を行う過程の中で取り込む．すなわち，具体的には，新たな梁要素（9節点梁要素）の考案とペナルティ法の適用により仮定を取り込んでいる．ティモシェンコ梁理論の仮定を用いると，一般にせん断剛性が過大評価される．そのため，ここでは，せん断補正係数を構成則に導入する．このような定式化の流れ，およびそれにより得られる有限要素方程式は，節点変数に回転角を含まないこともあり，簡潔でわかりやすいものとなっている．本定式化の妥当性は，数値計算例により検証する．